OncoTargets and Therapy

Dovepress

open access to scientific and medical research

Open Access Full Text Article

ORIGINAL RESEARCH

RETRACTED ARTICLE: MYO5A inhibition by miR-145 acts as a predictive marker of occult neck lymph node metastasis in human laryngeal squamous cell carcinoma

This article was published in the following Dove Press journal:
OncoTargets and Therapy

Xudong Zhao[1]
Wei Zhang[2]
Wenyue Ji[1]

[1]Department of Otorhinolaryngology, Shengjing Hospital, China Medical University, Shenyang, China; [2]Department of Endocrinology, Shengjing Hospital, China Medical University, Shenyang, China

Introduction: Each year, ~50,000 patients worldwide die of laryngeal squamous cell carcinoma (LSCC) because of its highly metastatic property. However, its pathogenic mechanisms are still unclear, and in particular, the prediction of metastasis remains inconclusive. This study aimed to define the role of microRNA-145 (miR-145) in LSCC progression. We also aimed to elucidate the clinical significance of the miR-145/MYO5A pathway, especially the predictive function of MYO5A in neck lymph node metastasis.

Materials and methods: MYO5A and miR-145 expression was analyzed in 132 patients with LSCC, and association between their expression and clinicopathological features were evaluated. We validated the regulatory relationship between miR-145b and MYO5A by dual luciferase reporter assay. The role of the miR-145/MYO5A pathway in proliferation, metastasis, and apoptosis was examined in vitro. The predictive functions of MYO5A in neck lymph node metastasis and prognosis were confirmed according to patient follow-up.

Results: Our results showed downregulation of miR-145 in LSCC, which was negatively correlated with MYO5A suppression of LSCC progression and metastasis. MiR-145 directly regulated MYO5A expression in vitro and suppressed LSCC proliferation and invasion while promoting apoptosis by inhibiting MYO5A.

Conclusion: Notably, overexpression of serum MYO5A in LSCC predicted cervical nodal occult metastasis and poor prognosis, providing an effective indicator for predicting neck lymph node metastasis and assessing LSCC prognosis.

Keywords: laryngeal squamous cell carcinoma, miR-145, MYO5A, laryngeal cancer

Introduction

Laryngeal carcinoma is one of the most common carcinomas of the head and neck. Its occurrence ranks third among head and neck malignancies, accounting for 3.1%–8.1% of these cancers.[1] Laryngeal squamous cell carcinoma (LSCC) accounts for more than 90% of laryngeal carcinomas.[2] Established treatments such as radiation, chemotherapy, and surgery can have little effect on advanced cases.[3–6] Owing to its aggressive nature and the limitations of early neck lymph node metastasis detection methods, there has not been significant improvement in the 5-year survival rate of patients with LSCC over the past 20 years.[7] Poor prognosis is usually associated with cervical nodal occult metastasis, which cannot be detected by clinical examination before treatment. Therefore, it is necessary to identify suppressive and predictive biomarkers for cervical nodal occult metastasis to improve the diagnosis and treatment of patients with LSCC.

MicroRNA-145 (miR-145) was first identified in the heart tissue of mice and later reported in humans.[8,9] MiR-145 is located within a 4.09 kb region on

Correspondence: Wenyue Ji
Department of Otorhinolaryngology, Shengjing Hospital, China Medical University, No 36 Sanhao Street, Heping District, Shenyang 110004, China
Tel +86 24 96615 61311
Email jiwenyueent@hotmail.com

submit your manuscript | www.dovepress.com
Dovepress
http://dx.doi.org/10.2147/OTT.S164597

human chromosome 5 (5q32–33). It negatively regulates gene expression posttranscriptionally by binding to sites in the 3′ untranslated region (UTR) of target mRNAs.[10] It is among the most downregulated miRNAs in a variety of cancers, including bladder cancer,[11,12] breast cancer,[13,14] colon cancer,[9,15] colorectal cancer,[16–19] gastric cancer,[20] hepatocellular carcinoma,[21,22] lung cancer,[23,24] nasopharyngeal carcinoma,[25] oral cancer,[26] ovarian cancer,[27,28] pituitary tumors,[29] and prostate cancer.[30] MiR-145 has a strong inhibitory effect on cancer cell proliferation and is considered a tumor suppressor. It also suppresses the nodal metastasis of various solid malignancies, including cervical small-cell carcinoma, hepatocellular carcinoma, and colorectal carcinoma.[31–33] The effects of miR-145 on LSCC development and metastasis remain unknown.

A target gene predictive assay was performed using online target prediction tools (TargetScan, miRWalk, and PicTar). The genes predicted by all the software were considered as potential candidates. Combined with previous research, MYO5A may be a candidate target gene of miR-145. Class V myosins-like MYO5A are actin-dependent motor proteins that are primarily involved in the intracellular transport of organelles.[34] Early studies of MYO5A focused on its roles in neuron formation and function and neurological disease.[35–41] MYO5A also plays an important role in malignant melanoma.[42–45] Lan et al implicated MYO5A in cancer metastasis, and showed that MYO5A expression was increased in a number of highly metastatic cancer cell lines and metastatic colorectal cancer tissues.[46] Mendez et al revealed that expression of MYO5A is associated with neck lymph node metastasis of oral squamous cell carcinoma and, in combination with three other genes, is a better predictive marker of neck lymph node metastasis than primary tumor size.[47] Recently, Dynoodt et al observed decreased MYO5A mRNA and protein in miR-145 overexpressing melanoma cells.[48] However, the functions and clinical significance of MYO5A in LSCC neck lymph node metastasis are still unknown.

In this study, we demonstrate that miR-145 suppresses human LSCC progression and metastasis by inhibiting MYO5A, and that the serum MYO5A level may be an effective predictor of neck lymph node metastasis and patient prognosis.

Materials and methods

Study subjects and patient tissue samples

A total of 132 patients with LSCC who underwent total laryngectomy at Shengjing Hospital were included in this study (Table S1). Fresh tissue and blood samples were prospectively collected. Normal laryngeal mucosa tissue samples were collected from 57 of the 132 patients. Written informed consent was obtained from all participants, and the Ethics Committee of Shengjing Hospital approved the study (2014PS17K). Overall survival (OS) time was defined as the interval between the date of surgery and the date of death or last follow-up. Patient follow-up was maintained until either death or the cutoff date (November 2016). Clinicopathological data were obtained before initial treatment. Outcomes were tracked by telephone or from outpatient care records.

Enzyme-linked immunosorbent assay (ELISA)

A commercial ELISA kit (MyBioSource, San Diego, CA, USA) was used to survey serum MYO5A levels according to the manufacturer's instructions. Fasting venous blood (1 mL) was extracted and centrifuged to isolate serum, which was stored at −80°C. Anti-MYO5A antibody (Thermo Fisher Scientific, Waltham, MA, USA) was used to coat 96-well plates overnight at 4°C. Serum samples and reconstituted standards (100 µL) were loaded in duplicate and incubated at 37°C for 2 h. After three washes, the wells were subsequently incubated with Detection Reagent A for 1 h at room temperature. After seven washes, the wells were incubated with Detection Reagent B (horseradish peroxidase-conjugated avidin) for 60 min at room temperature. Antigen-antibody complexes were revealed by adding 3,3′,5,5′-tetramethylbenzidine and measuring the absorbance at 450 nm.

Quantitative real-time PCR analysis

Total miRNAs were isolated from fresh tissues and cells using the mirVanaTM miRNA Isolation kit (Thermo Fisher) according to the manufacturer's instructions. After cDNA synthesis, miR-145 expression levels were analyzed using the mirVanaTM miRNA Isolation kit (Thermo Fisher) and run on a 7300 real-time PCR system (Thermo Fisher). Reaction conditions included an initial 2 min incubation at 95°C, then 40 cycles at 95°C for 8 s, and 60°C for 40 s. Data were analyzed by the $2^{-\Delta\Delta CT}$ method. The average value of the control group was set to 1, and all relative values were multiplied by 10. The primer sequences used are listed in Box 1.[49]

Western blot analysis

Total proteins were extracted from Hep-2 cells and tissues and quantitated by the Bradford method. The proteins were separated by sodium dodecyl sulfate-polyacrylamide gel electrophoresis on 8% gels and transferred to polyvinylidene difluoride membranes. The membranes were blocked with

Box 1 The primer sequences of Q-PCR

U6	RT:CGACTCGATCCAGTCTCAGGGTCCGAGGT ATTCGATCGAGTCGCACTTTTTTTTTTTTV Forward: 5′-CTCGCTTCGGCAGCACA-3′ Reverse: 5′-AACGCTTCACGAATTTGCGT-3′
miR-145	RT:CGACTCGATCCAGTCTCAGGGTCCGAGGT ATTCGATCGAGTCGCACTTTTTTTTTTTTV Forward: 3′-TCCCTAAGGACCCTTTTGACC-5′ Reverse: 5′-AGTCTCAGGGTCCGAGGTATTC-3′

5% skim milk for 1 h at room temperature, incubated with primary antibodies overnight at 4°C, washed with tris-buffered saline containing 0.5‰ TWEEN 20 (TBST) three times, incubated with secondary antibodies for 2 h at room temperature, and washed with TBST three times. Primary antibodies for MYO5A (1:1,000) and β-actin (1:2,000) were obtained from Thermo Fisher. Proteins were visualized by enhanced chemiluminescence and imaged with a UVP Image System (BD Biosciences, San Jose, CA, USA). The densities of protein bands were determined using ImageJ software (BD Biosciences). The levels of MYO5A protein were expressed as (MYO5A protein grey scale value/β-actin value) ×100.

Cell culture and transient transfection

Human laryngeal carcinoma Hep-2 cells and TU177 cells (from the Shanghai Cell Bank of the Chinese Academy of Sciences, China) were maintained in a complete Roswell Park Memorial Institute (RPMI)-1640 medium containing 10% fetal bovine serum (FBS), L-glutamine (2 mmol/L), salt pyruvate (1 mmol/L), 1% nonessential amino acids, and streptomycin (10 mg/L) at 37°C in a humidified atmosphere of 5% CO_2. Hep-2 cells (3×10^4) were transfected with miR-145 mimic, MYO5A-specific siRNA, a MYO5A overexpression vector (Cyagen Biosciences Inc., Santa Clara, CA, USA), or their negative controls (NCs; Thermo Fisher) in 6-well plates using Lipofectamine® 2000 transfection reagent (Thermo Fisher). After 48 h of transfection, cells were harvested for further assays.

Flow cytometry

Live Hep-2 cells (10^6 cells) were fixed and permeabilized (BD Biosciences) then stained with an anti-MYO5A antibody (Thermo Fisher) for 20–30 min on ice. Next, cells were incubated with phycoerythrin-conjugated secondary antibody (Thermo Fisher) for 30 min on ice. Flow cytometry was performed on an LSR II flow cytometer (BD Biosciences) and the results were analyzed with FlowJo software (BD Biosciences).

Quantification of apoptotic cells

An Annexin-V Apoptosis kit (BD Biosciences) was used to determine the extent of apoptosis. Cells were collected and incubated with 7-aminoactinomycin D (7-AAd) and annexin-V antibody for 15 min at room temperature. Flow cytometry was performed on an LSR II flow cytometer (BD Biosciences) and analyzed with FlowJo software (BD Biosciences). Annexin V and 7-AAd double positive cells were considered apoptotic. Annexin V positive/7-AAd negative cells were considered to be in early apoptosis.

Cell proliferation assays

Cells were treated with 10 μg/mL mitomycin for 2 h, and then their proliferation was evaluated by MTT assay (Sigma-Aldrich Co., St Louis, MO, USA). After transient transfection, cells were harvested and cultured in 96-well plates at 37°C in a humidified atmosphere with 5% CO_2 for 24, 48, 72, and 96 h. At each time interval, 5 mg/mL MTT was added to each well and the cells were incubated for 4 h. The blue formazan products formed were dissolved in dimethyl sulfoxide (100 μL) and spectrophotometrically measured at 490 nm.

Cell migration and invasion assays

Cells were treated with 10 μL/mL mitomycin for 2 h before migration and invasion assays. Cell migration assays were performed in triplicate using Transwell migration chambers (8 μm pore size; Corning Incorporated, Corning, NY, USA). For invasion assays, wells were coated with diluted extracellular matrix (ECM) solution (Sigma-Aldrich Co.) as described in the manufacturer's protocol. After transfection, Hep-2 cells (5×10^4) were transferred to the upper chamber or ECM gel in serum-free culture. RPMI-1640 containing 10% FBS was added to the lower chambers. After incubation at 37°C and 5% CO_2 for 24 h, cells that remained on top of the filter were removed and cells that migrated or invaded to the lower surface were fixed in 90% ethanol, stained with H&E, and counted by light microscopy.

Colorimetric caspase-3 assays

Hep-2 and TU177 cells were lysed, and their protein concentrations were determined. Proteins (100 μg) were treated with 10 μL of Ac-DEVD-pNA (Abcam, Cambridge, MA, USA) and incubated for 2 h at 37°C. The absorbance at 405 nm was measured using a microplate reader (Bio-Tek Instruments Inc., Winooski, VT, USA).

Luciferase reporter assays

The 3′-UTR region of human *MYO5A* was cloned into the pGL3 luciferase reporter plasmid (Promega Corporation, Fitchburg, WI, USA). Wild type and mutated *MYO5A* 3′ UTR luciferase reporter vectors were cotransfected into Hep-2 cells with miR-145 mimic or an NC using Lipofectamine 2000™ (Thermo Fisher).[50] Cells were harvested 48 h after transfection. Luciferase activities were analyzed using the Dual-Luciferase Reporter Assay System (Promega Corporations) according to the manufacturer's protocol.

Patient follow-up

All patients were examined in our outpatient department every 3 months for the first 2 years after resection and semi-annually thereafter. Follow-up included history taking, cervical computed tomography (CT) scans, and laryngoscopy. Radionuclide bone scans, brain CT scan, and chest positron emission tomography-CT scans were conducted if clinically indicated. The survival time was defined as the interval between surgery and death or last follow-up. We defined 36 months as the minimum follow-up period for accepting a case as N_0.

Statistical analysis

All experiments were repeated in triplicate. The data represent the mean±SD. All statistical analyses were performed using SPSS statistical software package (version 17; SPSS Inc., Chicago, IL, USA) Student's *t*-test was used to compare differences in miR-145 and MYO5A expression between LSCC and healthy mucosa tissues. Correlations between miR-145 expression, MYO5A expression, and clinicopathological parameters were also analyzed by *t*-test. The Pearson correlation test was used to analyze the relationship between miR-145 and MYO5A expression. A receiver operating characteristic (ROC) curve and its area under the curve (AUC) were introduced to evaluate the predictive value of serum MYO5A levels. The Kaplan–Meier method was used to compare patient survival. For all analyses, we considered *P*-values <0.05 to be significant.

Results

Downregulation of miR-145 in LSCC is negatively correlated with MYO5A expression

To investigate miR-145 expression in LSCC, quantitative real-time PCR was performed on 132 LSCC samples and 57 healthy laryngeal mucosa samples acquired from patients with LSCC who underwent total laryngectomy. MiR-145 expression significantly decreased in the LSCC group compared with that in the healthy mucosa group (4.05±2.82 vs 10.00±2.44, P=0.002; Figure 1A). MiR-145 expression decreased significantly in 49/57 LSCC tissues compared with that in paired healthy mucosa tissues (P<0.001; Figure 1B). Western blot was used to detected MYO5A expression in the 132 LSCC samples and 57 laryngeal normal mucosa samples (Figure 1C). The relative MYO5A expression value in LSCC tissue was 64.52±15.20, significantly higher than that in healthy tissue (31.81±8.30, P=0.007). MYO5A expression was also compared among the 57 paired LSCC and mucosa tissues (Figure 1D), and it increased significantly in 52/57 LSCC samples (P < 0.001). The correlation between miR-145 and MYO5A levels in the LSCC and control samples was evaluated by Pearson correlation test. We found that miR-145 expression was negatively correlated with MYO5A expression (r=0.549, P=0.018; Figure 1E). These results suggest that the aberrant expression of miR-145 and MYO5A correlated in clinical LSCC samples.

MiR-145 may suppress LSCC progression and metastasis in humans

To explore the clinical significance of the miR-145/MYO5A pathway in LSCC, we extracted clinicopathological parameters for the 132 patients from inpatient records. Age, sex, primary tumor site, T stage, tumor cell differentiation, and neck lymph node metastasis were analyzed for association with miR-145 and MYO5A levels (Tables 1 and 2). There were no significant differences in miR-145 and MYO5A levels with different ages, sexes, and primary tumor sites. Notably, miR-145 expression was significantly increased in early T stages and with good cell differentiation. In addition, patients suffering from neck lymph node metastasis (including neck lymph node metastasis and occult neck lymph node metastasis) displayed lower miR-145 expression. In contrast, MYO5A expression was suppressed significantly at early T stages but was unchanged by cell differentiation status. Furthermore, marked increases in MYO5A expression were observed in patients with neck lymph node metastasis. The relationship between miR-145 and MYO5A expression levels in tumors with perinodal versus lymphovascular and perineural invasion, as confirmed during surgery, were analyzed (Tables 1 and 2). Patients with perinodal invasion displayed higher MYO5A expression. Other differences were not statistically significant. Taken together, the results suggest that miR-145 may suppress LSCC progression and metastasis by regulating MYO5A expression.

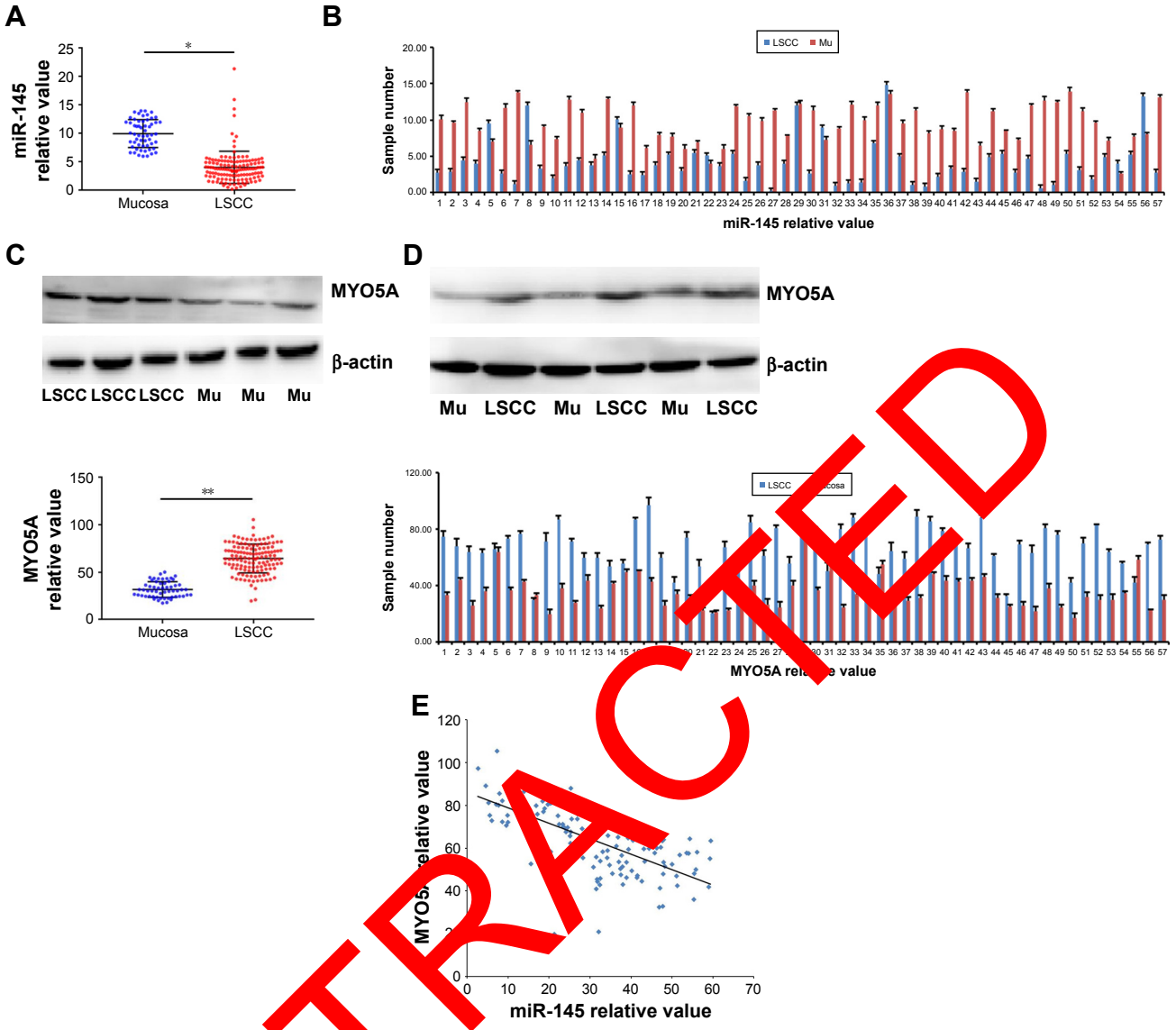

Figure 1 Downregulation of miR-145 in LSCC is negatively correlated with MYO5A expression (**A**). Quantitative real-time PCR was performed on 132 LSCC samples and 57 laryngeal healthy Mu acquired from patients with LSCC who underwent total laryngectomy. (**B**) MiR-145 expression in 57 paired LSCC and healthy Mu tissues. (**C**) Western blot was used to detected MYO5A expression differences between LSCC and healthy Mu. (**D**) MYO5A expression in 57 paired tissue samples. (**E**) The Pearson correlation test was used to analyze the relationship between miR-145 and MYO5A levels.

Notes: *$P<0.05$; **$P<0.01$.

Abbreviations: LSCC, laryngeal squamous cell carcinoma; Mu, mucosa; miR-145, microRNA-145.

MiR-145 directly regulates MYO5A expression in Hep-2 cells

We predicted that MYO5A might be a miR-145 candidate target using online target predication tools (TargetScan, miRWalk, and PicTar). In addition, Dynoodt et al reported decreased MYO5A mRNA and protein in miR-145-overexpressing melanoma cells.[48] However, whether miR-145 regulates MYO5A remains unresolved. We transfected Hep-2 cells with miR-145 mimic or an NC and western blot was used to detect MYO5A expression (Figure 2A). MYO5A decreased significantly in Hep-2 cells transfected with miR-145 mimic (from 71.35±4.61 to 39.25±2.69, $P<0.001$) but was unaffected by the negative control (68.16±2.82). This suggests that MYO5A expression changed in correlation with miR-145 levels. Flow cytometry was used to detect the MYO5A mean fluorescence intensity (MFI) in Hep-2 cells transfected with miR-145 mimic. The MFI decreased significantly compared with that of the NC (Figure 2B). In contrast, there was no significant difference in the expression of nudix hydrolase 1 (NUDT1), a potential miR-145 target in Hep-2 cells, with changes in miR-145 expression ($P>0.05$; Figure 2C).

Table 1 Correlation of miR-145 expression with the clinicopathological features of patients with LSCC

Parameters	Patients n (%)	miR-145 level	*P*-value
Total	132		
Sex			0.408
Male	114 (86.4)	4.14±2.98	
Female	18 (13.6)	3.54±1.58	
Age (years)			0.343
≥60	84 (63.6)	3.88±2.07	
<60	48 (36.4)	4.36±3.82	
Primary site			0.671
Glottic	76 (57.6)	3.96±2.42	
Supraglottic	56 (42.4)	4.18±3.32	
T stage			0.021
T_2	51 (38.6)	5.13±3.80	
T_3 T_4	81 (61.4)	3.38±1.69	
Differentiation			0.013
High	85 (64.4)	4.68±3.19	
Moderate and low	47 (35.6)	2.93±1.47	
Neck lymph node metastasis			0.005
N+	61 (46.2)	2.85±1.41	
N–	71 (53.8)	5.09±3.31	
Perinodal invasion			0.588
+	21 (45.7)	3.87±2.53	
–	25 (54.3)	4.30±2.97	
Lymphovascular and perineural invasion			0.495
+	13 (28.3)	3.73±3.01	
–	33 (71.7)	4.28±2.85	

Note: The data is presented as mean ± SD.
Abbreviations: LSCC, laryngeal squamous cell carcinoma; miR-145, microRNA-145.

Table 2 Correlation between MYO5A expression and the clinicopathological features of patients with LSCC

Parameters	Patients n (%)	MYO5A level	*P*-value
Total	132		
Sex			0.883
Male	114 (86.4)	64.60±15.22	
Female	18 (13.6)	64.03±15.52	
Age (years)			0.864
≥60	84 (63.6)	64.35±15.21	
<60	48 (36.4)	64.83±15.35	
Primary site			0.952
Glottic	76 (57.6)	64 [illegible]	
Supraglottic	56 (42.4)	[illegible]4.62±14.8[illegible]	
T stage			0.003
T_2	51 (38.6)	[illegible]60±14.40	
T_3 T_4	81 (6[illegible])	67.[illegible]14.96	
Differentiation			0.713
High	8[illegible]64.4)	64.78±14.95	
Moderate and low	47 (3[illegible])	6[illegible]±14.09	
Neck lymph node [illegible]stasis			
N+	61 (46.2)	73.02±12.39	
N–	[illegible] (53.8)	57.23±13.57	
Perinod[illegible]invasion			0.037
+	21 (45.7)	69.23±18.81	
–	25 (54.3)	60.17±16.79	
Lymp[illegible]ascular and [illegible]rineural invasion			0.274
+	13 (28.3)	66.39±16.51	
	33 (71.7)	63.11±15.88	

N[illegible]: The[illegible]a is presented as mean ± SD.
[illegible]bbreviation: LSCC, laryngeal squamous cell carcinoma.

To confirm the regulatory relationship betw[illegible]n miR-[illegible]5 and MYO5A, we conducted luciferase repor[illegible] assay[illegible]uciferase reporters containing wild type or mu[illegible]d *MYO5A* [illegible]O5Auta were constructed (Figure 2D). The relative [illegible]ciferase activity of the reporter containing the wi[illegible]type *MYO5A* [illegible]UTR was significantly decreased with [illegible]R-145 [illegible]otransfection ($P<0.001$), whereas the activity o[illegible]e re[illegible]rter containing the mutant binding site was u[illegible]ffected ([illegible]ure 2E). These results strongly indicate that M[illegible]O5A [illegible]a direc[illegible]t of miR-145.

MiR-145 [illegible]ppresses LSCC proliferation and invasion [illegible]nd promotes apoptosis by inhibiting MYO[illegible]A expression

The effects of miR-145/MYO5A levels on LSCC growth were examined by cell proliferation assay. Hep-2 cells were transiently transfected with miR-145 mimic and either MYO5A-specific siRNA or an NC siRNA. Hep-2 cells with overexpression of miR-145 or knockdown of MYO5A displayed time-dependent reductions in cell proliferation compared with the NCs (Figure 3A and B), indicating that miR-145 inhibits proliferation via MYO5A in vitro. MiR-145 overexpression decreased proliferation by [illegible]9.4%±3.5%, 29.7%±4.7%, 32.6%±3.1%, and 33.5%±4.5% after 24, 48, 72, and 96 h, respectively ($P=0.046$), whereas MYO5A siRNA decreased proliferation by 20.1%±1.6%, 28.1%±2.3%, 22.2%±1.7%, and 27.5%±2.7% after 24, 48, 72, and 96 h, respectively ($P=0.044$).

To determine the effects of miR-145/MYO5A levels on LSCC migration and invasion, we conducted Transwell migration and invasion assays. Overexpression of miR-145 or knockdown of MYO5A in Hep-2 cells resulted in reduced cell migration and invasion (Figure 3C and D). Annexin-V staining was used to examine the effects of miR-145/MYO5A on LSCC apoptosis. Overexpression of miR-145 significantly promoted Hep-2 cell apoptosis (Figure 3E), as did knockdown of MYO5A (Figure 3F). Similar results were observed by colorimetric caspase 3 assay (Figure 3G and H). Collectively, these data indicate that miR-145 suppresses LSCC proliferation and invasion and promotes apoptosis in vitro by inhibiting MYO5A.

Forced MYO5A overexpression restores the inhibitory effects of miR-145

To further understand the MYO5A-mediated inhibitory effects of miR-145 in LSCC, we transfected an MYO5A

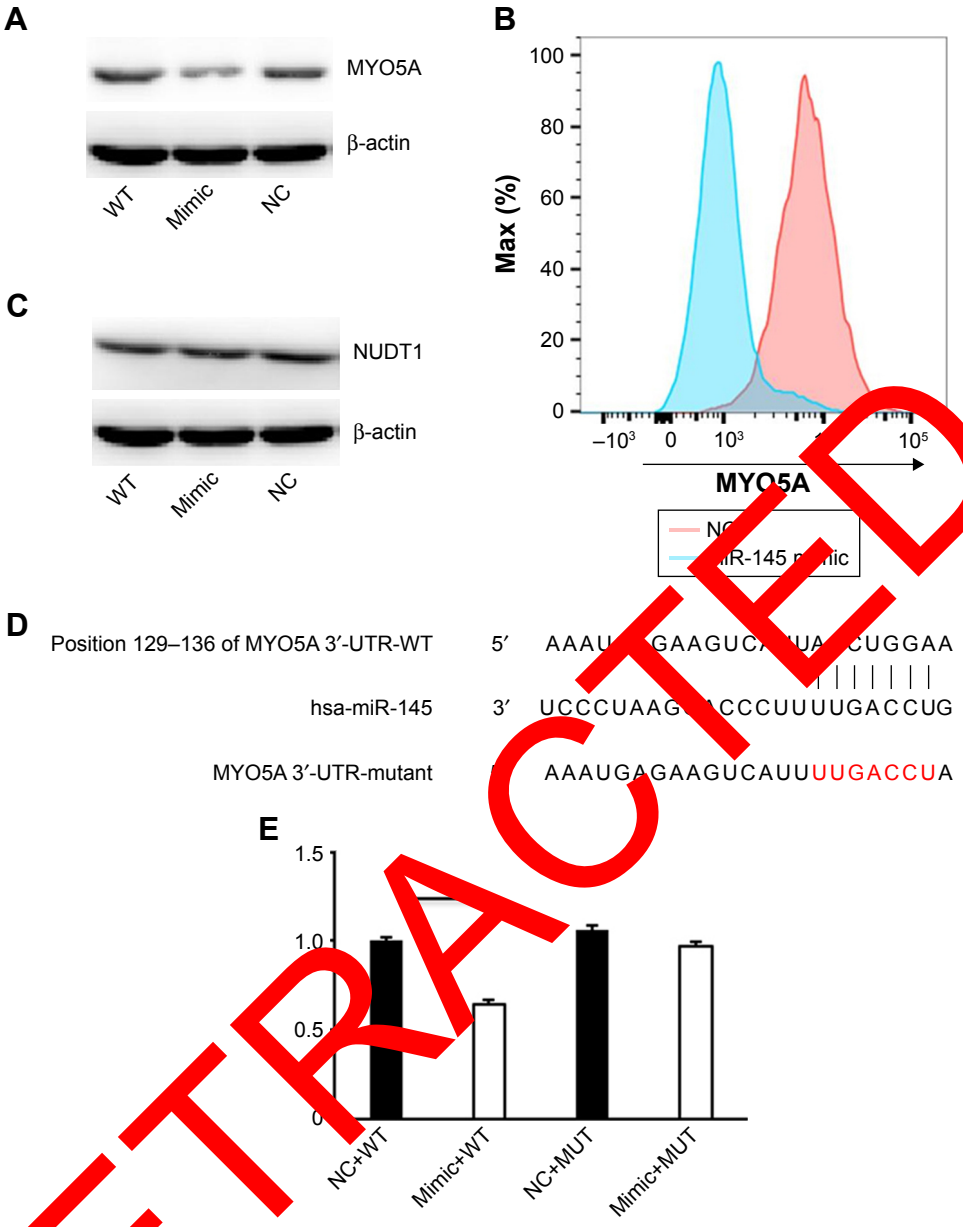

Figure 2 MiR-145 directly regulates MYO5A expression in Hep-2 cells. (**A**) Western blot analysis of MYO5A levels in Hep-2 after transfection of either miR-145 mimic or an NC. (**B**) Representative graph and MFI of MYO5A staining in Hep-2 cells. (**C**) NUDT1 expression in Hep-2 cells transfected with miR-145 mimic or an NC. (**D**) MiR-145 directly interacts with the 3′-UTR of MYO5A. (**E**) Luciferase reporter assays were performed 48 h after transfection with WT or MUT *MYO5A* 3′-UTR plasmids cotransfected with miR-145 mimic or NC.
Note: *P<0.001.
Abbreviations: NC, negative control; MFI, mean fluorescence intensity; WT, wild type; MUT, mutant; NUDT 1, nudix hydrolase 1; miR-145, microRNA-145.

overexpression vector into miR-145-overexpressing TU177 cells (Figure 4A) restoring MYO5A expression (69.71±5.77 vs 40.03±4.62 in cells transfected with mimic alone; P=0.031), and found that MYO5A overexpression released the suppressive effects of miR-145 on proliferation and invasion (Figure 4B and C). Compared with miR-145-overexpressing TU177 cells, a time-dependent increase in cell proliferation was observed in TU177 cells with MYO5A overexpression (6.8%±0.4%, 18.4%±2.7%, 22.0%±4.1%, and 30.3%±4.7% at 24, 48, 72, and 96 h, respectively, P<0.05). Moreover, MYO5A overexpression significantly inhibited apoptosis (Figure 4D and E). These finding suggest that miR-145 suppresses LSCC progression by inhibiting MYO5A.

MYO5A overexpression in LSCC predicts cervical nodal occult metastasis

Cervical nodal occult metastasis is a form of neck lymph node metastasis that cannot be detected by clinical examination, including physical and radiological tests. Many N_0 stage patients who suffer from cervical nodal occult metastasis

do not receive proper treatment in time because of a lack of effective predictive indicators. To explore the utility of MYO5A levels in predicting cervical occult metastasis, western blot and ELISA were used to detect MYO5A expression in LSCC tissues and serum. We divided the 132 patients into 3 groups according to cervical metastatic state, N^+, N_0^+, and N^-, which contained 29, 32, and 71 patients, respectively. Patients with recognized neck lymph node metastasis before surgery were defined as N^+. The N_0^+ group included patients that were initially recognized as neck lymph node metastasis negative before surgery but were diagnosed with neck lymph node metastasis either during surgery or in later follow-up. The N^- group included patients in which neck lymph node metastasis was not detected at any point in the process.

Western blot was used to detect MYO5A expression in 132 LSCC tissues. MYO5A increased significantly in the N^+ and N_0^+ groups compared with that in the N^- group (74.69±10.63 vs 57.23±13.57, P=0.008; 71.50±13.79 vs 57.23±13.57, P=0.024; Figure 5A), whereas the N^+ and N_0^+ groups showed similar MYO5A expression (Figure 5B). These results revealed that MYO5A could be used as an indicator of neck lymph node metastasis, and suggest that the cervical treatment plan (cervical lymph node dissection or radiotherapy) for each patient could be determined according to preoperative assessment of MYO5A expression. However, in clinical practice, western blot is not typically used in presurgical bi[illegible]rker detection. To determine more easily MYO[illegible]A expre[illegible]ion before surgery, ELISA was used to dete[illegible]serum MYO[illegible]A levels. The serum concentrations [illegible] MYO[illegible] in the [illegible] and N_0^+ groups were significantl[illegible]igher th[illegible]n tho[illegible]i[illegible]the N^- group (294.2±62.0 pg/mL [illegible]199.[illegible]±71.1 pg/mL, P=0.003;

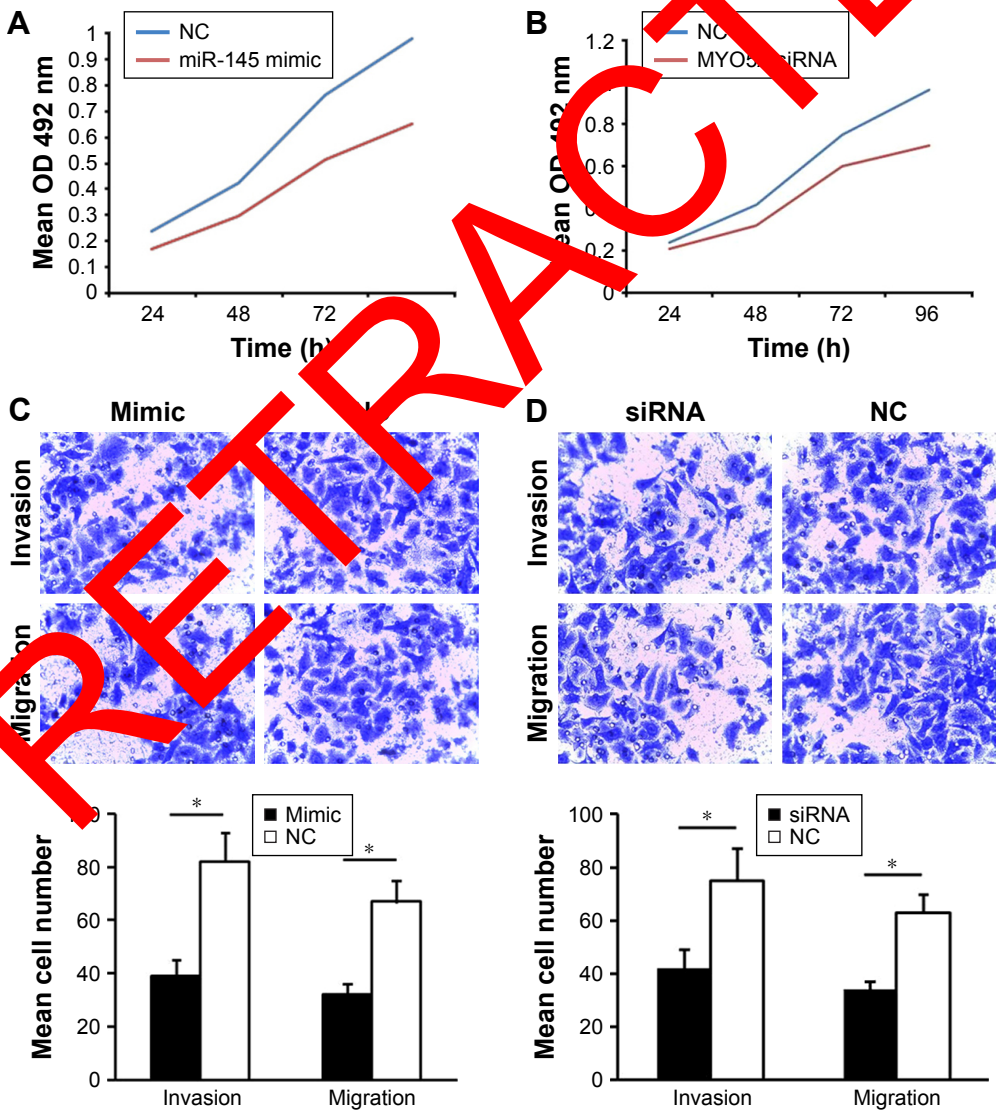

Figure 3 (*Continued*)

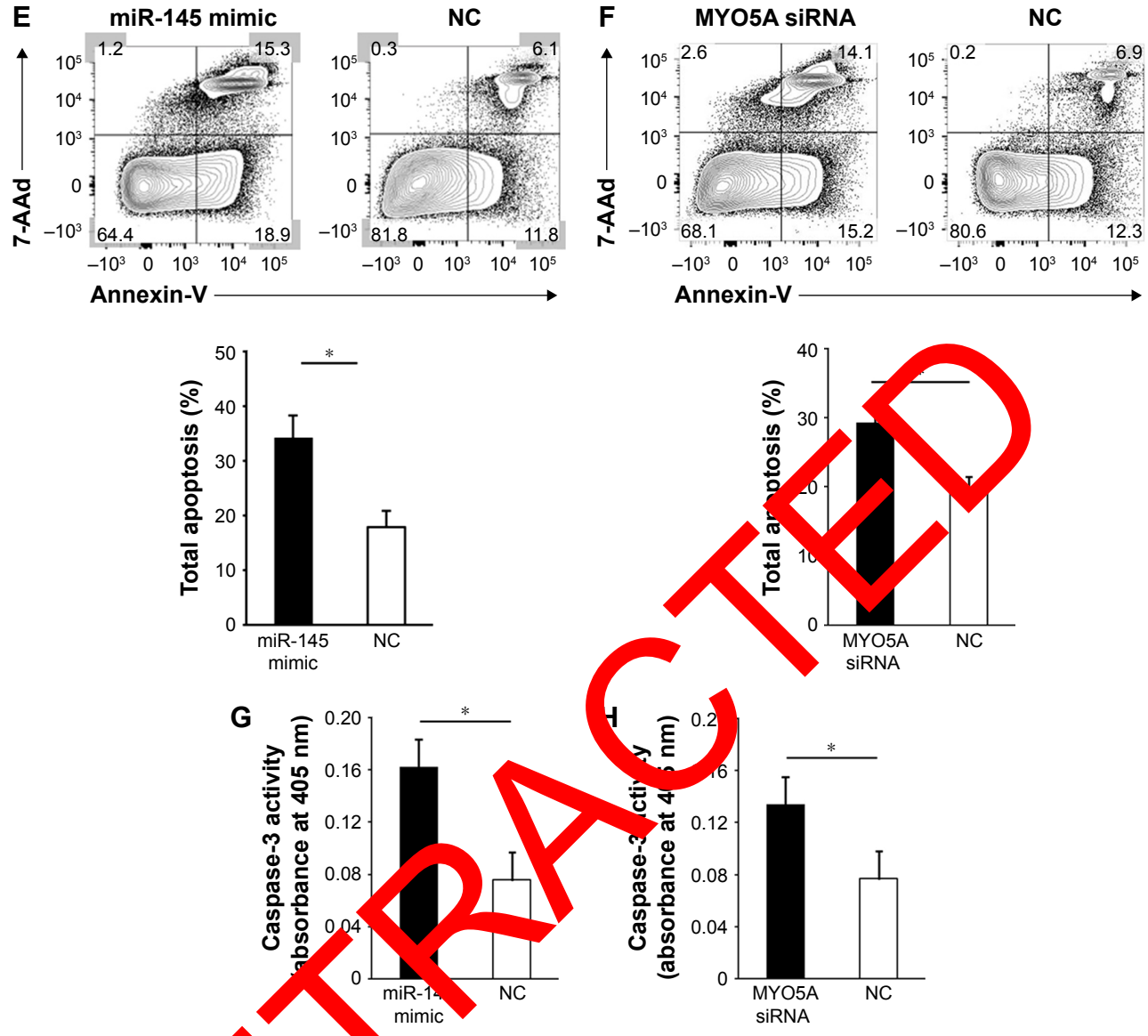

Figure 3 MiR-145 suppresses LSCC proliferation and invasion and promotes apoptosis by inhibiting MYO5A. (**A**) Proliferation rates of Hep-2 cells at various time points after transfection with either miR-145 mimic or an NC. (**B**) Proliferation rates of Hep-2 cells at various time points after transfection with either MYO5A siRNA or an NC. (**C**) Hep-2 cells were transiently transfected with miR-145 mimic or an NC and subjected to migration and invasion assays. Representative photographs and quantification are shown. Magnification: ×200. (**D**) Hep-2 cells were transiently transfected with MYO5A-specific or NC siRNA and subjected to migration and invasion assays. Representative photographs and quantification are shown. Magnification: ×200. (**E**) Representative graph of the percentage of Hep-2 cells in apoptosis after transfection with miR-145 mimic or an NC. (**F**) Representative graph of the percentage of Hep-2 cells in apoptosis after transfection with MYO5A-specific siRNA or an NC. (**G**) Caspase-3 activity in Hep-2 cells transfected with miR-145 mimic or an NC. (**H**) Caspase-3 activity in Hep-2 cells transfected with MYO5A-specific siRNA or an NC.
Note: *P<0.05.
Abbreviations: LSCC, laryngeal squamous cell carcinoma; NC, negative control; miR-145, microRNA-145; 7-AAd, 7-aminoactinomycin D; OD, optical density.

276.3±73.5 pg/mL vs 199.3±71.1 pg/mL, P=0.009; Figure 5C), with no significant differences between the N^+ and N_0^+ groups (Figure 5D). Taken together, these results suggest that MYO5A levels in both the primary tumor tissue and the serum increase significantly with neck lymph node or occult metastasis, indicating its promise as a presurgical biomarker.

An ROC curve was drawn to determine the best serum MYO5A concentration for neck lymph node metastasis prediction. The AUC was calculated to evaluate the diagnostic value of MYO5A expression. The AUC of serum MYO5A to predict neck lymph node metastasis was 0.823. The diagnostic sensitivity (77.8%) and specificity (75.4%) were highest when the cutoff value was 240.5 pg/mL, suggesting the best predictive performance at this level (Figure 5E). We conclude that MYO5A can be a powerful indicator for predicting neck lymph node metastasis, especially cervical occult metastasis, in clinical practice, enabling the planning of suitable therapies for neck lymph node metastasis-negative patients.

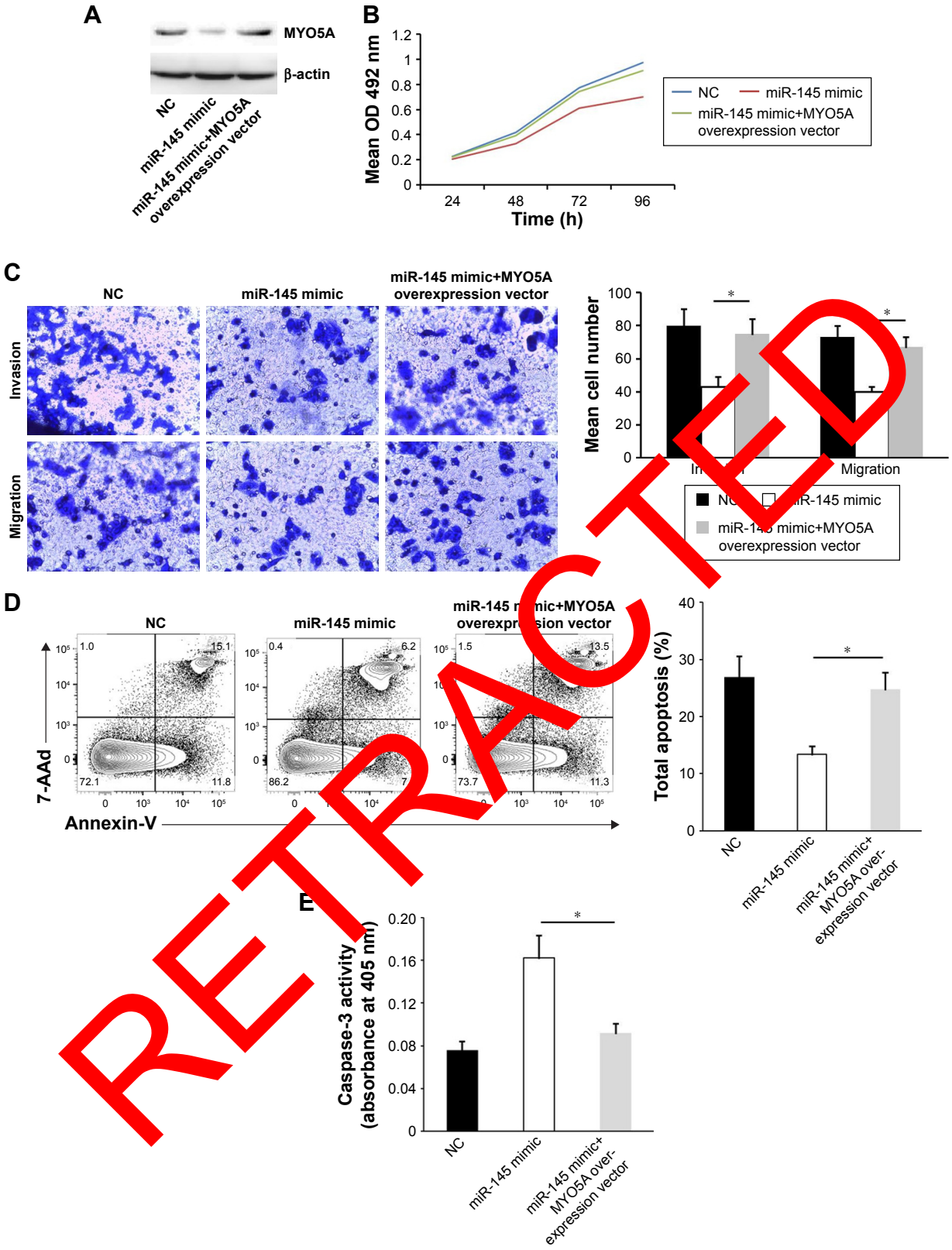

Figure 4 MYO5A overexpression restores the inhibitory effects of miR-145. (**A**) Representative Western blot showing the restoration of MYO5A expression after cotransfection of a miR-145 mimic and an MYO5A overexpression vector compared with cells transfected with miR-145 mimic alone. (**B**) Proliferation rates of miR-145-overexpressing TU177 cells at various time points after MYO5A overexpression. (**C**) Representative photographs (top; ×200 magnification) and quantitative analysis (bottom) of Transwell migration and invasion assays in TU177 cells transfected with miR-145 mimic with and without MYO5A overexpression. (**D**) Representative graph of the percentage of TU177 cells in apoptosis after transfection with miR-145 mimic with and without MYO5A overexpression. (**E**) Caspase-3 activity of TU177 cells transfected with miR-145 mimic with and without MYO5A overexpression.

Note: *$P<0.05$.

Abbreviations: LSCC, laryngeal squamous cell carcinoma; NC, negative control; miR-145, microRNA-145; OD, optical density.

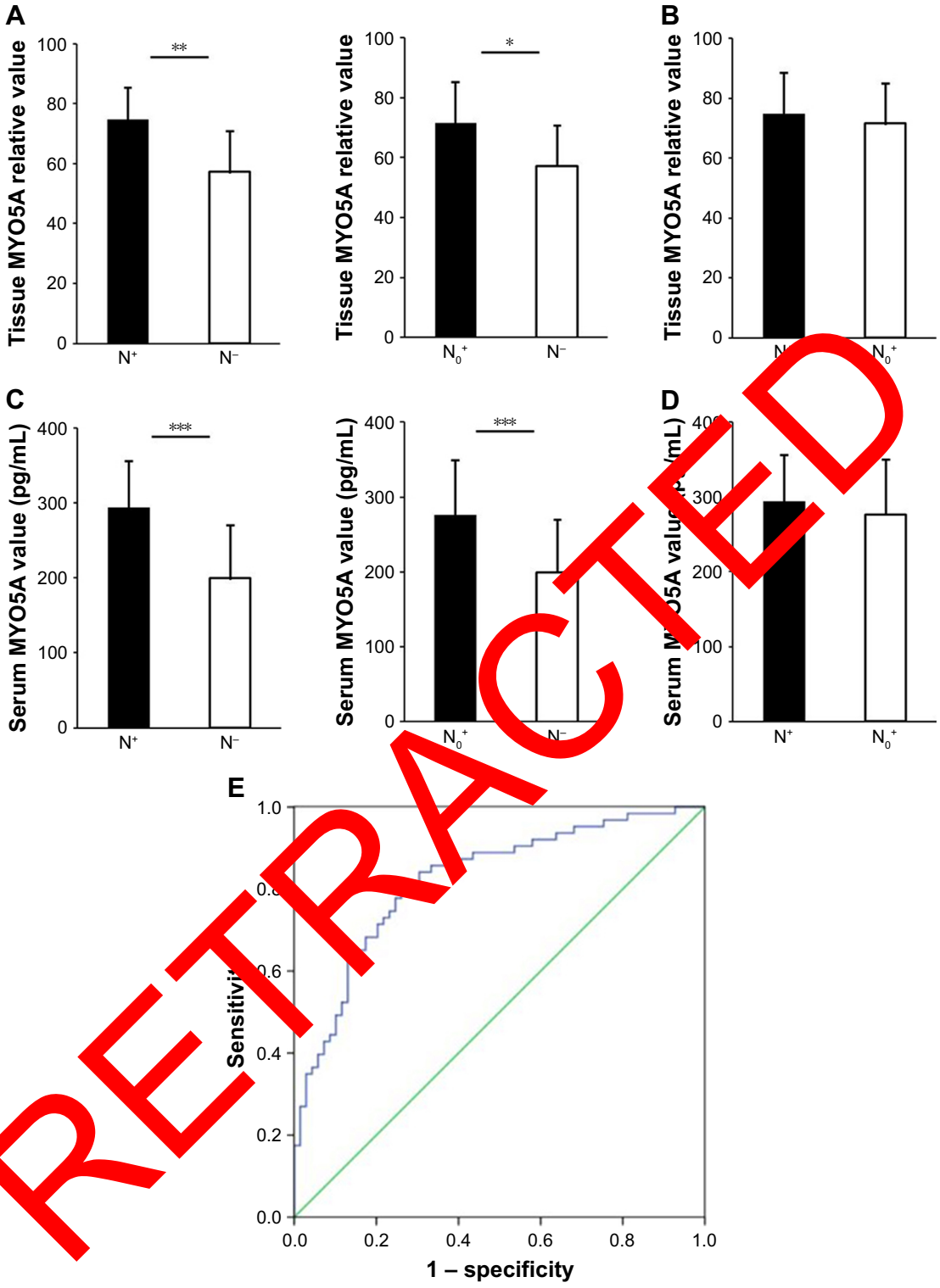

Figure 5 Overexpression of MYO5A in LSCC predicts cervical nodal occult metastasis (**A**, **B**) MYO5A protein levels in the N^+, N_0^+, and N^- groups. (**C**, **D**) Serum MYO5A concentrations in the N^+, N_0^+, and N^- groups. (**E**) ROC curve of the neck lymph node metastasis predictive value of MYO5A levels in patients with LSCC.
Notes: *$P<0.05$, **$P<0.01$, ***$P<0.001$.
Abbreviations: LSCC, laryngeal squamous cell carcinoma; ROC, receiver operating characteristic.

MYO5A overexpression predicts poor prognosis

All 132 patients were followed-up at our outpatient clinic or by telephone. The mean follow-up time was 70 months (median: 72 months; range: 38–93 months). The 3- and 5-year OS rates were 77.27% and 71.21%, respectively. The patients were divided into 2 groups according to miR-145 or serum MYO5A levels. Patients with lower miR-145 levels (<4.05)

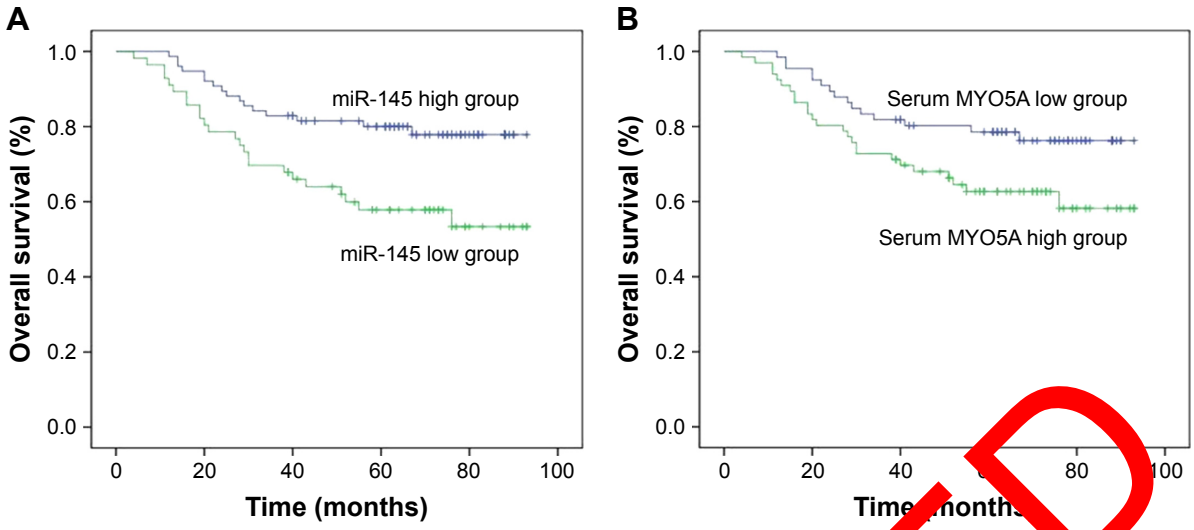

Figure 6 Overexpression of MYO5A predicts poor prognosis (**A**) OS rates after 3 and 5 years with varying miR-145 levels. (**B**) OS rates after 3 and 5 years with varying serum MYO5A levels.
Abbreviations: miR-145, microRNA-145; OS, overall survival.

had significantly poorer 3- and 5-year OS rates (69.64% vs 82.89% and 58.93% vs 80.2%, respectively, *P*=0.027; Figure 6A). Patients with higher serum MYO5A levels (>240.5 pg/mL) also had significantly poorer 3- and 5-year OS rates (72.31% vs 82.09% and 64.62% vs 77.61%, respectively, *P*=0.041; Figure 6B).

Next, univariate and multivariate analyses were conducted to determine potential prognostic factors. Only parameters that were significant in univariate analyses were further analyzed by multivariate analysis. Univariate analysis showed that differentiation (*P*=0.018), T stage (*P*=0.023), neck lymph node metastasis status (*P*=0.029), miR-145 level (*P*=0.041) and serum MYO5A level (*P*=0.021) had significant effects on OS (Table 3). Only the T stage (*P*=0.047), cervical state (*P*=0.029), and serum MYO5A level (*P*=0.038) were independent significant prognostic factors for OS in multivariate analysis (Table 3). This suggests that pretreatment examination of the serum MYO5A level could provide powerful evidence for prognosis assessment and individual therapeutic planning.

Discussion

Laryngeal cancer is the 11th most common malignancy in the world.[51] Its treatment is becoming more effective due to developments in surgery and radiotherapy, but there has not been any significant improvement in the 5-year survival rate of patients with LSCC over the past 20 years.[7] Cervical nodal metastasis, especially occult metastasis, is generally responsible for poor outcomes.[52] Therefore, we were eager to identify an indicator of neck lymph node metastasis that could be used to assess the clinical prognosis of LSCC.

The suppressive functions of miR-145 are well documented in many solid malignancies,[11–28] but until now, its role in LSCC has not been determined. The functions of MYO5A in the development of cardiovascular system are well reported,[53] and several investigations have focused on

Table 3 Evaluation of potential prognostic factors for LSCC

Characteristic	Univariate analysis			Multivariate analysis		
	HR	95% CI	*P*-value	HR	95% CI	*P*-value
Sex	0.455	0.140–1.475	0.189	–	–	–
Age	0.770	0.411–1.442	0.414	–	–	–
Primary location	1.580	0.849–2.940	0.149	–	–	–
Differentiation	**0.393**	**0.181–0.853**	**0.018**	0.450	0.201–1.008	0.052
T stage	**1.505**	**0.960–2.007**	**0.023**	**1.461**	**0.981–1.995**	**0.047**
Neck lymph node metastasis	**1.815**	**1.038–3.142**	**0.003**	**1.629**	**1.004–2.314**	**0.029**
MiR-145 level	**0.621**	**0.327–1.102**	**0.041**	0.662	0.298–1.004	0.194
Serum MYO5A level	**1.592**	**0.992–2.138**	**0.021**	**1.631**	**1.013–2.417**	**0.038**
Tissue MYO5A level	**1.941**	**0.879–3.244**	**0.148**	–	–	–

Note: Statistically significant factors are shown in bold.
Abbreviations: LSCC, laryngeal squamous cell carcinoma; miR-145, microRNA-145.

the role of MYO5A in malignant melanoma.[41–44] Studies have also revealed that MYO5A is associated with metastasis.[45,46] Dynoodt et al found decreased MYO5A mRNA and protein in miR-145 overexpressing melanoma cells[48] but did not demonstrate a regulatory relationship between miR-145 and MYO5A. In addition, the functions and regulatory mechanisms of MYO5A in LSCC proliferation and neck lymph node metastasis are not well defined. In the present study, aberrant expression of miR-145 and MYO5A were observed in 132 LSCC tissues, with an inverse correlation between their levels. Moreover, the clinicopathological parameters of the 132 patients were extracted from inpatient records to explore the functions of miR-145 and MYO5A in human LSCC development. T stage, cell differentiation, and cervical metastatic state were recognized as factors affected by miR-145 expression. MYO5A expression was associated with the T stage and cervical metastatic state. This revealed the possibility that miR-145 suppresses the progression and metastasis of human LSCC by inhibiting MYO5A, and this was confirmed in vitro. We transfected Hep-2 cells with miR-145 mimic and MYO5A-specific siRNA. Hep-2 cells with miR-145 overexpression showed decreased MYO5A expression, proliferation, and invasion but increased apoptosis. Similar results were obser[illegible] Hep-2 cells with knockdown of MYO5A. Luciferase reporter assays demonstrated the regulatory relation[illegible]ip betw[illegible] miR-145 and MYO5A, indicating that mi[illegible]-145 s[illegible]ppress[illegible] the proliferation and invasion of He[illegible]2 cells [illegible]directly suppressing MYO5A expression. [illegible] our k[illegible]wledge, this is the first study that indicates th[illegible]iR-145 ca[illegible]uppress the development of human LSC[illegible] by ta[illegible]eting MYO5A.

In addition, we also d[illegible]covered that s[illegible]um MYO5A levels are a valuable predi[illegible]or of cer[illegible]ical nodal occult metastasis, and can be used to [illegible]sess [illegible]ognosis. Cervical nodal occult metastasis is i[illegible]isible [illegible] clinical [illegible]amination (eg, physical examinati[illegible]n or C[illegible] scan) [illegible]e surgery or radiotherapy. When [illegible]k lym[illegible]e metastasis occurs after treatment, the salvage su[illegible]y is always difficult and often has little success. It is therefore [illegible]ucial to find a clinically useful indicator to predict occult n[illegible]ck lymph node metastasis. Mendez et al reported the use of a 4-gene model (MYO5A, ring finger protein 145, F-box protein 32, and CTONG2002744) as a predictive indicator for cervical nodal metastasis.[47] These results provide the possibility of predicting cervical nodal occult metastasis, but the method has not been widely adapted in clinical practice. We detected serum MYO5A levels using ELISA, which is very common in clinical practice. In addition, we defined cervical nodal metastasis during follow-up for at least 3 years rather than simply during surgery, which highlighted the important predictive value of serum MYO5A levels. The AUC demonstrated the promise of this method for use in clinical practice. Serum MYO5A levels can be simply measured before surgery or radiotherapy, enabling the formation of suitable therapy plans for neck lymph node metastasis-negative patients.

Collectively, we demonstrated that miR-145 suppresses human LSCC progression and metastasis by inhibiting MYO5A. Serum MYO5A may be an effective predictor of neck lymph node metastasis and patient prognosis. H[illegible]wever, a trial with 132 samples is not large enough to c[illegible]nfirm the p[illegible]dictive ability of serum MYO5A levels. Further c[illegible]nical trials w[illegible] larger sample sizes will be required to [illegible]nfirm th[illegible] conclusi[illegible]n.

Acknowledgment

This study w[illegible] suppo[illegible] by the [illegible]ational Natural Science Foundatio[illegible] China (No 8[illegible]64). This funding played an important role i[illegible] experimental conduction, data collection, and [illegible] analysis.

Disclosure

The authors [illegible]port no conflicts of interest in this work.

References

1. Mourad WF, Hu KS, Shourbaji RA, Dolan J, Blakaj DM, Shasha D, Harrison LB. Exploration of the role of radiotherapy in the management of early glottic cancer with complete carotid artery occlusion. *Onkologie*. 2013;36:433–435.
2. Markou K, Christoforidou A, Karasmanis I, et al. Laryngeal cancer: Epidemiological data from Northern Greece and review of the literature. *Hippokratia*. 2013;17:313–318.
3. Yu X, Wu Y, Liu Y, Deng H, Shen Z, Xiao B, Guo J. miR-21, miR-106b and miR-375 as novel potential biomarkers for laryngeal squamous cell carcinoma. *Curr Pharm Biotechnol*. 2014;15(5):503–508.
4. Hu A, Huang JJ, Xu WH, et al. miR-21 and miR-375 microRNAs as candidate diagnostic biomarkers in squamous cell carcinoma of the larynx: association with patient survival. *Am J Transl Res*. 2014;6(5):604–613.
5. Liu J, Lei DP, Jin T, Zhao XN, Li G, Pan XL. Altered expression of miR-21 and PTEN in human laryngeal and hypopharyngeal squamous cell carcinomas. *Asian Pac J Cancer Prev*. 2011;12(10):2653–2657.
6. Wu TY, Zhang TH, Qu LM, et al. MiR-19a is correlated with prognosis and apoptosis of laryngeal squamous cell carcinoma by regulating TIMP-2 expression. *Int J Clin Exp Pathol*. 2014;7(1):56–63.
7. Lothaire P, de Azambuja E, Dequanter D, et al. Molecular markers of head and neck squamous cell carcinoma: Promising signs in need of prospective evaluation. *Head Neck*. 2006;28(3):256–269.
8. Lagos-Quintana M, Rauhut R, Lendeckel W, Tuschl T. Identification of novel genes coding for small expressed RNAs. *Science*. 2001; 294(5543):853–858.
9. Michael MZ, O'Connor SM, van Holst Pellekaan NG, Young GP, James RJ. Reduced accumulation of specific microRNAs in colorectal neoplasia. *Mol Cancer Res*. 2003;1(12):882–891.
10. Bagga S, Bracht J, Hunter S, Massirer K, Holtz J, Eachus R, Pasquinelli AE. Regulation by let-7 and lin-4 miRNAs. Results in target mRNA degradation. *Cell*. 2005;122(4):553–563.

11. Ichimi T, Enokida H, Okuno Y, et al. Identification of novel microRNA targets based on microRNA signatures in bladder cancer. *Int J Cancer*. 2009;125(2):345–352.
12. Dyrskjøt L, Ostenfeld MS, Bramsen JB, et al. Genomic profiling of microRNAs in bladder cancer: miR-129 is associated with poor outcome and promotes cell death in vitro. *Cancer Res*. 2009;69(11):4851–4860.
13. Iorio MV, Ferracin M, Liu CG, et al. MicroRNA gene expression deregulation in human breast cancer. *Cancer Res*. 2005;65(16):7065–7070.
14. Sempere LF, Christensen M, Silahtaroglu A, et al. Altered MicroRNA expression confined to specific epithelial cell subpopulations in breast cancer. *Cancer Res*. 2007;67(24):11612–11620.
15. Schepeler T, Reinert JT, Ostenfeld MS, et al. Diagnostic and prognostic microRNAs in stage II colon cancer. *Cancer Res*. 2008;68(15): 6416–6424.
16. Bandres E, Cubedo E, Agirre X, et al. Identification by real-time PCR of 13 mature microRNAs differentially expressed in colorectal cancer and non-tumoral tissues. *Mol Cancer*. 2006;5:29.
17. Slaby O, Svoboda M, Fabian P, et al. Altered expression of miR-21, miR-31, miR-143 and miR-145 is related to clinicopathologic features of colorectal cancer. *Oncology*. 2007;72(5–6):397–402.
18. Wang CJ, Zhou ZG, Wang L, et al. Clinicopathological significance of microRNA-31, -143 and -145 expression in colorectal cancer. *Dis Markers*. 2009;26(1):27–34.
19. Motoyama K, Inoue H, Takatsuno Y, et al. Over- and under-expressed microRNAs in human colorectal cancer. *Int J Oncol*. 2009;34(4): 1069–1075.
20. Takagi T, Iio A, Nakagawa Y, Naoe T, Tanigawa N, Akao Y. Decreased expression of microRNA-143 and -145 in human gastric cancers. *Oncology*. 2009;77(1):12–21.
21. Gramantieri L, Ferracin M, Fornari F, et al. Cyclin G1 is a target of miR-122a, a microRNA frequently down-regulated in human hepatocellular carcinoma. *Cancer Res*. 2007;67(13):6092–6099.
22. Varnholt H, Drebber U, Schulze F, Wedemeyer I, Schirmacher P, Dienes HP, Odenthal M. MicroRNA gene expression profile of hepatitis C virus-associated hepatocellular carcinoma. *Hepatology*. 2008;47(4): 1223–1232.
23. Liu X, Sempere LF, Galimberti F, et al. Uncovering growth-suppressive MicroRNAs in lung cancer. *Clin Cancer Res*. 2009;15(4):1177–1183.
24. Cho WC, Chow AS, Au JS. Restoration of tumour suppressor miR-145 inhibits cancer cell growth in lung adenocarcinoma patients with epidermal growth factor receptor mutation. *Eur J Cancer*. 2009;45(12): 2197–2206.
25. Chen H-C, Chen G-H, Chen Y-H, et al. MicroRNA deregulation and pathway alterations in nasopharyngeal carcinoma. *Br J Cancer*. 2009; 100(6):1002–1011.
26. Yu T, Wang XY, Gong RG, et al. The expression profile of microRNAs in a model of 7,12-dimethylbenz[a]anthrance-induced oral carcinogenesis in Syrian hamster. *J Exp Clin Cancer Res*. 2009;28(1):64.
27. Iorio MV, Visone R, Leva G, et al. MicroRNA signatures in human ovarian cancer. *Cancer Research*. 2007;67(18):8699–8707.
28. Nam EJ, Yoon H, Kim SW, et al. MicroRNA expression profiles in serous ovarian carcinoma. *Clin Cancer Res*. 2008;14(9):2690–2695.
29. Amaral FC, Torres N, Saggioro F, et al. MicroRNAs differentially expressed in ACTH-secreting pituitary tumors. *J Clin Endocrinol Metab*. 2009;94(1):320–323.
30. Ozen M, Creighton CJ, Ozdemir M, Ittmann M. Widespread deregulation of microRNA expression in human prostate cancer. *Oncogene*. 2008; 27(12):1788–1793.
31. Huang L, Lin JX, Yu YH, Zhang MY, Wang HY, Zheng M. Downregulation of six microRNAs is associated with advanced stage, lymph node metastasis and poor prognosis in small cell carcinoma of the cervix. *PLoS One*. 2012;7(3):e33762.
32. Zhang L, Xiang ZL, Zeng ZC, Fan J, Tang ZY, Zhao XM. A microRNA-based prediction model for lymph node metastasis in hepatocellular carcinoma. *Oncotarget*. 2016;7(3):3587–3598.
33. Yuan W, Sui C, Liu Q, Tang W, An H, Ma J. Up-regulation of microRNA-145 associates with lymph node metastasis in colorectal cancer. *PLoS One*. 2014;9(7):e102017.
34. Li JF, Nebenführ A. The tail that wags the dog: the globular tail domain defines the function of myosin V/XI. *Traffic*. 2008;9(3):290–298.
35. Griscelli C, Durandy A, Guy-Grand D, Daguillard F, Herzog C, Prunieras M. A syndrome associating partial albinism and immunodeficiency. *Am J Med*. 1978;65(4):691–702.
36. Pastural E, Barrat FJ, Dufourcq-Lagelouse R, et al. Griscelli disease maps to chromosome 15q21 and is associated with mutations in the myosin-Va gene. *Nature genetics*. 1997;16(3):289–292.
37. Bahadoran P, Ortonne JP, Ballotti R, de Saint-Basile G. Comment on Elejalde syndrome and relationship with Griscelli syndrome. *Am J Med Genet A*. 2003;116A(4):408–409.
38. Ménasché G, Ho CH, Sanal O, et al. Griscelli syndrome restricted to hypopigmentation results from a melanophilin defect (GS3) or a MYO5A F-exon deletion (GS1). *J Clin Invest*. 2003;112(3):450–456.
39. Prekeris R, Terrian DM. Brain myosin V is a synaptic vesicle-associated motor protein: evidence for a Ca^{2+}-dependent interaction with the synaptobrevin–synaptophysin complex. *J Cell Biol*. 1997;137(7): 1589–1601.
40. Costa MC, Mani F, Santos W Jr, Espreafico EM, Larson RE. Brain myosin-V, a calmodulin-carrying myosin, binds to calmodulin-dependent protein kinase II and activates its kinase activity. *J Biol Chem*. 1999; 274:15811–15817.
41. Takamori S, Holt M, Stenius K, et al. Molecular anatomy of a trafficking organelle. *Cell*. 2006;127(4):831–846.
42. Fernandez LP, Milne RL, Pita G, et al. Pigmentation-related genes and their implication in malignant melanoma susceptibility. *Exp Dermatol*. 2009;18(7):634–642.
43. Neves CP, Moraes MH, Sousa JF, et al. Myosin-Va contributes to manifestation of malignant-related properties in melanoma cells. *J Invest Dermatol*. 2013;133(12):2809–2812.
44. Isidoro-Toledo TC, Borges AC, Araújo DD, et al. A myosin-Va tail fragment sequesters dynein light chains leading to apoptosis in melanoma cells. *Cell Death Dis*. 2013;4(3):e547.
45. Fernandez-Perez MP, Montenegro MF, Saez-Ayala M, Sanchez-del-Campo L, Pinero-Madrona A, Cabezas-Herrera J, Rodriguez-Lopez JN. Suppression of antifolate resistance by targeting the myosin Va trafficking pathway in melanoma. *Neoplasia*. 2013;15(7):826–839.
46. Lan L, Han H, Zuo H, et al. Upregulation of myosin Va by Snail is involved in cancer cell migration and metastasis. *Int J Cancer*. 2010;126(1): 53–64.
47. Mendez E, Lohavanichbutr P, Fan W, et al. Can a metastatic gene expression profile outperform tumor size as a predictor of occult lymph node metastasis in oral cancer patients? *Clin Cancer Res*. 2011;17(8): 2466–2473.
48. Dynoodt P, Speeckaert R, De Wever O, Chevolet I, Brochez L, Lambert J, Van Gele M. miR-145 overexpression suppresses the migration and invasion of metastatic melanoma cells. *Int J Oncol*. 2013; 42(4):1443–1451.
49. Zhan M, Zhao X, Wang H, et al. miR-145 sensitizes gallbladder cancer to cisplatin by regulating multidrug resistance associated protein 1. *Tumour Biol*. 2016;37(8):10553–10562.
50. Minami K, Taniguchi K, Sugito N, et al. MiR-145 negatively regulates Warburg effect by silencing KLF4 and PTBP1 in bladder cancer cells. *Oncotarget*. 2017;8(20):33064–33077.
51. Tomeh C, Holsinger FC. Laryngeal cancer. *Curr Opin Otolaryngol Head Neck Surg*. 2014;22(2):147–153.
52. Birkeland AC, Rosko AJ, Issa MR, et al. Occult nodal disease prevalence and distribution in recurrent laryngeal cancer requiring salvage laryngectomy. *Otolaryngol Head Neck Surg*. 2016;154(3):473–479.
53. Schumacher-Bass SM, Vesely ED, Zhang L, et al. Role for myosin-V motor proteins in the selective delivery of Kv channel isoforms to the membrane surface of cardiac myocytes. *Circ Res*. 2014;114:982–992.

Supplementary material

Table S1 The clinical parameters of all the LSCC patients

No	Gender	Age (years)	Primary location	Diagnosis	Cervical state	Differentiation	Surgical procedures
1	Male	49	Glottic	T2N0M0	N^-	High	Partial laryngectomy
2	Male	68	Supraglottic	T4N1M0	N^+	High	Total laryngectomy+bilateral neck dissections
3	Male	71	Glottic	T3N0M0	N^-	Moderate	Total laryngectomy
4	Male	54	Glottic	T2N0M0	N^-	High	Partial laryngectomy
5	Male	59	Supraglottic	T4N1M0	N^+	Moderate	Total laryngectomy+bilateral neck dissections
6	Male	64	Supraglottic	T3N0M0	N^-	High	Partial laryngectomy+unilateral neck dissections
7	Male	73	Supraglottic	T4N1M0	N^+	High	Total laryngecto[illegible]l neck dissections
8	Male	71	Glottic	T4N1M0	N^+	High	Total laryngec[illegible]my+bilatera[illegible]ck dissections
9	Female	52	Glottic	T3N0M0	N^-	Moderate	Total laryng[illegible]my
10	Male	65	Glottic	T3N0M0	N_0^+	High	Partial[illegible]y+bilateral[illegible]ck dissections
11	Male	72	Glottic	T4N1M0	N^+	Low	To[illegible]laryngectomy[illegible]ck dissections
12	Female	75	Glottic	T2N0M0	N^-	Low	[illegible]rtial lar[illegible]ctomy
13	Male	63	Glottic	T2N0M0	N^-	High	[illegible]ngectomy
14	Male	61	Glottic	T2N0M0	N^-	High	Parti[illegible]ryngect[illegible]y
15	Male	67	Glottic	T2N0M0	N_0^+	High	Total la[illegible]omy
16	Male	65	Glottic	T3N1M0	N^+	Moder[illegible]	Total laryngectomy+bilateral neck dissections
17	Male	73	Glottic	T2N0M0	N^-	High	[illegible]rtial laryngectomy
18	Female	75	Glottic	T2N0M0	N_0^+	[illegible]igh	Pa[illegible]al laryngectomy+bilateral neck dissections
19	Male	48	Glottic	T2N0M0	N_0^+	High	Partial laryngectomy+bilateral neck dissections
20	Male	47	Glottic	T3N0M0	N^-	High	Partial laryngectomy+bilateral neck dissections
21	Male	63	Glottic	T2N0M0	N^-	[illegible]igh	Partial laryngectomy
22	Male	65	Supraglottic	T3N1M0	[illegible]	M[illegible]	Total laryngectomy+bilateral neck dissections
23	Male	76	Glottic	T3N0M0	[illegible]	Moderate	Partial laryngectomy+unilateral neck dissections
24	Male	54	Supraglottic	T2N0M0	N[illegible]	[illegible]	Partial laryngectomy
25	Male	75	Glottic	T2[illegible]	N^-	High	Partial laryngectomy+bilateral neck dissections
26	Male	51	Glottic	[illegible]2N0M0	N^-	Moderate	Partial laryngectomy
27	Male	62	Supraglottic	T4N1M[illegible]	N^+	High	Total laryngectomy+bilateral neck dissections
28	Male	72	Glottic	[illegible]0	N^-	High	Total laryngectomy+unilateral neck dissections
29	Male	71	Supra[illegible]ttic	T2[illegible]0	N_0^+	Moderate	Partial laryngectomy+bilateral neck dissections
30	Female	47	G[illegible]ttic	T2N1M[illegible]	N_0^+	High	Partial laryngectomy+bilateral neck dissections
31	Male	65	Supraglotti[illegible]	T3N1M0	N_0^+	High	Partial laryngectomy+bilateral neck dissections
32	Male	62	Supraglottic	T3N1M0	N^+	High	Total laryngectomy+bilateral neck dissections
33	Male	65	Gl[illegible]ttic	T3N1M0	N^+	Low	Partial laryngectomy+bilateral neck dissections
34	Male	5[illegible]	[illegible]lottic	T3N0M0	N^-	High	Total laryngectomy+unilateral neck dissections
35	Male	58	Glottic	T2N0M0	N^-	High	Total laryngectomy
36	Male	[illegible]9	Supr[illegible]ottic	T3N1M0	N_0^+	Moderate	Partial laryngectomy+bilateral neck dissections
37	M[illegible]	[illegible]	[illegible]praglottic	T3N0M0	N_0^+	Moderate	Total laryngectomy+bilateral neck dissections
38	[illegible]	[illegible]	Glottic	T4N3M0	N^+	High	Total laryngectomy+bilateral neck dissections
39	Male	77	Glottic	T2N0M0	N^-	Moderate	Partial laryngectomy
40	Male	59	Glottic	T3N0M0	N_0^+	Moderate	Partial laryngectomy+unilateral neck dissections
41	Male	[illegible]0	Glottic	T2N1M0	N^+	High	Partial laryngectomy+bilateral neck dissections
42	Male	66	Glottic	T2N0M0	N^-	Moderate	Partial laryngectomy
43	Male	42	Supraglottic	T3N0M0	N^-	High	Total laryngectomy+unilateral neck dissections
44	Male	46	Glottic	T3N0M0	N^-	Moderate	Total laryngectomy
45	Male	46	Supraglottic	T2N0M0	N^-	High	Partial laryngectomy+bilateral neck dissections
46	Male	54	Glottic	T2N0M0	N^-	High	Partial laryngectomy+unilateral neck dissections
47	Male	76	Supraglottic	T2N1M0	N_0^+	High	Partial laryngectomy+bilateral neck dissections
48	Male	65	Glottic	T2N0M0	N^-	High	Partial laryngectomy
49	Male	48	Supraglottic	T3N1M0	N^+	Low	Total laryngectomy+bilateral neck dissections
50	Female	78	Glottic	T3N1M0	N_0^+	High	Partial laryngectomy+bilateral neck dissections

(*Continued*)

Table S1 (*Continued*)

No	Gender	Age (years)	Primary location	Diagnosis	Cervical state	Differentiation	Surgical procedures
51	Female	56	Glottic	T3N0M0	N^-	High	Total laryngectomy
52	Male	75	Supraglottic	T3N0M0	N^-	Moderate	Partial laryngectomy+unilateral neck dissections
53	Male	70	Supraglottic	T2N1M0	N^+	Moderate	Partial laryngectomy+bilateral neck dissections
54	Male	60	Supraglottic	T3N0M0	N^-	High	Total laryngectomy+unilateral neck dissections
55	Male	77	Glottic	T3N0M0	N^-	Low	Total laryngectomy
56	Male	80	Supraglottic	T3N1M0	N_0^+	High	Total laryngectomy+bilateral neck dissections
57	Male	74	Glottic	T2N0M0	N^-	Low	Partial laryngectomy
58	Male	66	Supraglottic	T3N0M0	N^-	Moderate	Partial laryngectomy+unilateral neck dissections
59	Male	74	Glottic	T2N1M0	N_0^+	High	Partial laryngectomy+bilateral neck dissections
60	Male	50	Supraglottic	T3N1M0	N_0^+	Low	Total laryngectomy+bi[illegible] dissections
61	Male	47	Glottic	T3N0M0	N_0^+	High	Partial laryngectom[illegible]ilateral nec[illegible]issections
62	Male	76	Glottic	T3N0M0	N^-	High	Total laryngecto[illegible]nilateral neck[illegible]ssections
63	Male	53	Glottic	T4N1M0	N^+	Low	Total laryn[illegible]tomy+[illegible]teral neck [illegible]sections
64	Male	46	Supraglottic	T3N0M0	N^-	High	Partial l[illegible]ngectomy+uni[illegible]ral n[illegible]k dissections
65	Female	45	Glottic	T2N0M0	N^-	High	Parti[illegible]aryngect[illegible]y+bilater[illegible]eck dissections
66	Male	72	Glottic	T3N0M0	N^-	Moderate	T[illegible]ngec[illegible]omy+unila[illegible]ral neck dissections
67	Male	49	Glottic	T2N0M0	N^-	Low	Partial lar[illegible]ectomy
68	Male	60	Glottic	T3N0M0	N^-	High	Total laryngec[illegible]m[illegible]unilateral neck dissections
69	Male	69	Glottic	T2N1M0	N_0^+	Moderate	[illegible]tial laryngectomy+bilateral neck dissections
70	Male	67	Glottic	T4N2M0	N^+	High	Tota[illegible]ryngectomy+bilateral neck dissections
71	Female	47	Glottic	T2N0M0	N^-	Mo[illegible]ate	Partial l[illegible]ngectomy
72	Male	62	Glottic	T3N0M0	N^-	H[illegible]	Total laryngectomy+unilateral neck dissections
73	Male	51	Supraglottic	T4N1M0	N^+	H[illegible]	Total laryngectomy+bilateral neck dissections
74	Male	63	Glottic	T3N0M0	N^-	Hig[illegible]	Partial laryngectomy+unilateral neck dissections
75	Male	68	Supraglottic	T2N0M0	N^-	High	Partial laryngectomy
76	Female	74	Glottic	T4N1M0	N^+	[illegible]	Total laryngectomy+bilateral neck dissections
77	Male	36	Supraglottic	T2N0M0	N^-	[illegible]igh	Partial laryngectomy+bilateral neck dissections
78	Male	62	Glottic	T2N0M[illegible]	N_0^+	High	Partial laryngectomy+bilateral neck dissections
79	Female	56	Supraglottic	T2N[illegible]0	[illegible]	High	Partial laryngectomy+bilateral neck dissections
80	Male	54	Supraglottic	T[illegible]1M0	[illegible]	Low	Total laryngectomy+bilateral neck dissections
81	Male	62	Supraglottic	T3N[illegible]	N^-	High	Total laryngectomy+unilateral neck dissections
82	Male	80	Supraglotti[illegible]	T2N0M[illegible]	N^-	High	Partial laryngectomy+bilateral neck dissections
83	Male	63	Supra[illegible]tic	T4N2M0	N^+	High	Total laryngectomy+bilateral neck dissections
84	Female	70	Glottic	[illegible]N0M0	N^-	Moderate	Partial laryngectomy
85	Male	69	[illegible]praglottic	T4[illegible]M0	N^+	High	Total laryngectomy+bilateral neck dissections
86	Male	77	Glottic	T4N2M0	N^+	Low	Total laryngectomy+bilateral neck dissections
87	Male	80	Glo[illegible]	T4N1M0	N^+	Moderate	Total laryngectomy+bilateral neck dissections
88	Male	76	[illegible]ttic	T3N0M0	N_0^+	High	Partial laryngectomy+bilateral neck dissections
89	Male	79	S[illegible]praglot[illegible]	T4N1M0	N^+	Moderate	Total laryngectomy+bilateral neck dissections
90	Female	66	Glot[illegible]	T3N1M0	N_0^+	High	Total laryngectomy+bilateral neck dissections
91	Female	61	[illegible]ttic	T3N0M0	N^-	Moderate	Partial laryngectomy+unilateral neck dissections
92	Male	[illegible]	Supraglottic	T2N1M0	N_0^+	High	Partial laryngectomy+bilateral neck dissections
93	Female	[illegible]	Supraglottic	T3N0M0	N_0^+	High	Total laryngectomy+bilateral neck dissections
94	Male	74	Glottic	T3N0M0	N^-	High	Partial laryngectomy+unilateral neck dissections
95	Male	46	Supraglottic	T4N2M0	N^+	Low	Total laryngectomy+bilateral neck dissections
96	Male	57	Glottic	T3N0M0	N^-	High	Total laryngectomy
97	Male	66	Glottic	T2N1M0	N_0^+	High	Partial laryngectomy+bilateral neck dissections
98	Male	63	Glottic	T3N0M0	N^-	Moderate	Partial laryngectomy+unilateral neck dissections
99	Female	61	Supraglottic	T3N0M0	N^-	High	Total laryngectomy+unilateral neck dissections
100	Male	67	Glottic	T3N0M0	N^-	High	Partial laryngectomy+unilateral neck dissections
101	Female	70	Supraglottic	T2N1M0	N^+	Low	Partial laryngectomy+bilateral neck dissections
102	Male	50	Glottic	T3N0M0	N^-	Low	Total laryngectomy
103	Male	57	Supraglottic	T3N0M0	N^-	Moderate	Partial laryngectomy+unilateral neck dissections

(*Continued*)

Table S1 (*Continued*)

No	Gender	Age (years)	Primary location	Diagnosis	Cervical state	Differentiation	Surgical procedures
104	Male	47	Supraglottic	T3N0M0	N^-	High	Total laryngectomy+unilateral neck dissections
105	Male	64	Supraglottic	T3N1M0	N_0^+	Low	Partial laryngectomy+bilateral neck dissections
106	Male	71	Supraglottic	T2N0M0	N^-	High	Partial laryngectomy
107	Male	51	Supraglottic	T2N0M0	N^-	High	Partial laryngectomy+bilateral neck dissections
108	Male	70	Supraglottic	T4N1M0	N^+	Low	Total laryngectomy+bilateral neck dissections
109	Female	48	Supraglottic	T3N1M0	N_0^+	Low	Total laryngectomy+unilateral neck dissections
110	Male	67	Glottic	T2N0M0	N^-	High	Partial laryngectomy+bilateral neck dissections
111	Male	80	Glottic	T3N0M0	N_0^+	Low	Partial laryngectomy+bilateral neck dissections
112	Female	77	Glottic	T3N0M0	N_0^+	High	Total laryngectomy
113	Male	35	Glottic	T2N0M0	N^-	High	Partial laryngecto
114	Male	58	Glottic	T3N1M0	N^+	High	Total laryngec my+bilatera eck dissections
115	Male	45	Supraglottic	T3N2M0	N^+	High	Total laryng my+bilateral n k dissections
116	Male	76	Glottic	T3N1M0	N_0^+	High	Partial ryngect +bilateral ck dissections
117	Male	72	Supraglottic	T3N1M0	N_0^+	High	To laryngectomy ater eck dissections
118	Male	79	Glottic	T3N0M0	N^-	High	rtial lary ectomy+u teral neck dissections
119	Male	80	Supraglottic	T3N0M0	N^-	High	gectomy nilateral neck dissections
120	Male	57	Glottic	T2N0M0	N^-	High	Parti ryngect y
121	Male	64	Supraglottic	T2N0M0	N^-	High	Partial la omy+bilateral neck dissections
122	Male	52	Glottic	T2N0M0	N^-	Low	Partial laryngectomy
123	Male	56	Supraglottic	T3N0M0	N^-	High	rtial laryngectomy+unilateral neck dissections
124	Male	77	Glottic	T2N0M0	N^-	igh	Pa al laryngectomy
125	Male	50	Supraglottic	T3N0M0	N^-	High	Total laryngectomy+unilateral neck dissections
126	Male	52	Supraglottic	T2N0M0	N^-	High	Partial laryngectomy+unilateral neck dissections
127	Male	65	Supraglottic	T4N1M0	N^+	ow	Total laryngectomy+bilateral neck dissections
128	Male	58	Supraglottic	T3N1M0		Lo	Total laryngectomy+unilateral neck dissections
129	Male	76	Glottic	T3N0M0		High	Partial laryngectomy+unilateral neck dissections
130	Male	69	Supraglottic	T2N0M0	N	High	Partial laryngectomy+unilateral neck dissections
131	Male	47	Supraglottic	T2	N^-	High	Partial laryngectomy+bilateral neck dissections
132	Male	77	Glottic	2N0M0	N^-	High	Partial laryngectomy

Abbreviation: LSCC, laryngeal squamous cell carcino